GEOPHYSICAL RESEARCH LETTERS, VOL. 29, NO. 19, 1900, doi:10.1029/2002GL015581, 2002

Top-down estimate of a large source of atmospheric carbon monoxide associated with fuel combustion in Asia

Prasad Kasibhatla and Avelino Arellano
Nicholas School of the Environment and Earth Sciences, Duke University, Durham, NC, USA

Jennifer A. Logan and Paul I. Palmer
Division of Engineering and Applied Sciences, Harvard University, Cambridge, MA, USA

Paul Novelli
Climate Monitoring and Diagnostics Laboratory, NOAA, Boulder, CO, USA

Received 31 May 2002; revised 16 July 2002; accepted 8 August 2002; published 1 October 2002.

[1] Deriving robust regional estimates of the sources of chemically and radiatively important gases and aerosols to the atmosphere is challenging. Here, we focus on carbon monoxide. Using an inverse modeling methodology, we find that the source of carbon monoxide from fossil-fuel and biofuel combustion in Asia during 1994 was 350–380 Tg yr^{-1}, which is 110–140 Tg yr^{-1} higher than bottom-up estimates derived using traditional inventory-based approaches. This discrepancy points to an important gap in our understanding of the human impact on atmospheric chemical composition. *INDEX TERMS:* 0322 Atmospheric Composition and Structure: Constituent sources and sinks. **Citation:** Kasibhatla, P., et al., Top-down estimate of a large source of atmospheric carbon monoxide associated with fuel combustion in Asia, *Geophys. Res. Lett.*, *29*(19), 1900, doi:10.1029/2002GL015581, 2002.

1. Introduction

[2] Carbon monoxide (CO) is an important component of the atmospheric chemical system and has both natural and anthropogenic sources [*Logan et al.*, 1981]. Three-dimensional atmospheric chemical model (CTM) simulations using inventory-based bottom-up estimates of CO sources have shown that human activities contribute substantially to CO concentrations on regional and global scales [e.g., *Kanakidou and Crutzen*, 1999; *Granier et al.*, 1999; *Holloway et al.*, 2000; *Bey et al.*, 2001]. However, significant uncertainties persist in regional estimates of anthropogenic CO sources derived using bottom-up approaches, leading to corresponding uncertainties in the predicted human impacts on the atmospheric CO distribution. In a different approach, *Bergamaschi et al.* [2000] used an atmospheric CTM and surface measurements of atmospheric CO in an inverse modeling framework to derive estimates of CO emissions for various source categories. Here, we build on this inverse modeling approach by deriving geographically disaggregated estimates of anthropogenic CO sources.

[3] Our analysis consists of quantifying the CO sources from 11 source categories disaggregated by geographical region and source type. The 11 categories consist of 4 geographical categories used to represent fossil-fuel and-biofuel combustion sources in North America, Europe, Asia (including Indonesia and the Middle East), and Rest of the World (FF/BF-NA, FF/BF-EU, FF/BF-AS, and FF/BF-RW, respectively), 5 geographical categories used to represent biomass-burning sources in North America/Europe, Asia, Africa, Latin America, and Oceania (BB-NA/EU, BB-AS, BB-AF, BB-LA, and BB-OC, respectively), and 2 categories used to represent global CO chemical production from isoprene and monoterpenes (ISOP and TERP, respectively). In addition, we estimate the CO yield from methane (CH_4) oxidation (METH) as part of the inverse analysis.

0094-8276/02/2002GL015581$05.00

2. Methods

2.1. Inversion Methodology

[4] The inversion methodology consists of calculating a posteriori source estimates and uncertainties according using the equations [*Rodgers*, 2000]

$$\mathbf{x}' = \mathbf{x_a} + \mathbf{G}(\mathbf{y} - \mathbf{K}\mathbf{x_a}) \tag{1}$$

and

$$\mathbf{S}' = \left(\mathbf{K}^{\mathrm{T}}\mathbf{S}_\varepsilon^{-1}\mathbf{K} + \mathbf{S_a}^{-1}\right)^{-1}, \tag{2}$$

where, $\mathbf{y}$ is the measurement vector containing observed monthly-mean CO mixing ratios from all sites, $\mathbf{x_a}$ and $\mathbf{x}'$ are the state vectors containing a priori and a posteriori estimates of individual sources, $\mathbf{S_a}$ and $\mathbf{S}'$ are the a priori and a posteriori error covariance matrices, $\mathbf{S}_\varepsilon$ is the observation error covariance matrix, and $\mathbf{K}$ is the Jacobian matrix which describes the sensitivity of the measurement vector to finite changes in the state vector. The gain matrix $\mathbf{G}$ is given by

$$\mathbf{G} = \left(\mathbf{K}^{\mathrm{T}}\mathbf{S}_\varepsilon^{-1}\mathbf{K} + \mathbf{S_a}^{-1}\right)^{-1}\mathbf{K}^{\mathrm{T}}\mathbf{S}_\varepsilon^{-1}. \tag{3}$$

[5] Elements of $\mathbf{y}$ and $\mathbf{S}_\varepsilon$ are derived from a site-by-site analysis of ground-based atmospheric CO measurements from the NOAA/CMDL Cooperative Air Sampling Network [*Novelli et al.*, 1998]. At each site, monthly-mean concentrations for 1994 are derived from multi-year CO measurements using the smoothing procedure described by *Novelli et al.* [1998]. At most sites, the measurement records used in this study start between 1989 and 1992. At 6 sites, the records start in 1993/1994. All time series used here extend

through 1996. $\mathbf{S}_\varepsilon$ is assumed to be a diagonal matrix, with the individual diagonal elements representing the combined data uncertainty due to measurement as well as model errors. These elements are specified based on an analysis of the r.m.s. deviations of individual measurements from a specific month around the monthly-mean derived from the fitted curve. In order to minimize biases due to sparse measurements, individual measurements from 1993–95 are considered in calculating the r.m.s. statistics. Only months for which there are more than 3 individual measurements available for calculating the r.m.s. statistics are included in the analysis, and sites with less than 7 months of statistics are discarded to minimize biases due to incomplete data. In addition, we estimate that model biases are likely to be large at 3 sites (Baltic Sea; Cape Meares, Oregon; Key Biscayne, Florida) since these sites are in regions with large sources in the model, while the observational strategy employed was designed to measure the relatively clean background. Measurements from these sites are therefore not used in the analysis. The final data set consists of 419 monthly-means from 38 sites. For background sites as a whole, the 25th and 75th percentiles of the calculated r.m.s. deviations (expressed as a fraction of the corresponding monthly-mean) are 0.1 and 0.2, respectively. The corresponding 25th and 75th percentiles for sites in source regions are 0.15 and 0.3, respectively. Based on this analysis, minimum r.m.s. thresholds of 20% (for background sites) and 30% (for sites in source regions) of the corresponding monthly-means are used in specifying the diagonal elements of $\mathbf{S}_\varepsilon$.

[6] The yield of CO from CH_4 oxidation is solved in the inverse analysis. The a priori value of this parameter is set at 0.85 moles of CO produced per mole of CH_4 oxidized, with a 1-sigma uncertainty of ±0.05. For all other source categories, the a priori 1-sigma uncertainties are set at ±50% of the corresponding bottom-up source estimate, thereby weakly constraining the inverse solution with the a priori source estimates.

2.2. The Forward Model

[7] The Jacobian matrix **K** is specified using results from forward model calculations performed with the GEOS-CHEM global chemical transport model at a $4^\circ \times 5^\circ$ resolution driven by assimilated meteorological fields for 1994 [*Bey et al.*, 2001b]. Prescribed monthly-mean OH fields derived from a comprehensive tropospheric chemical simulation for 1994 [*Bey et al.*, 2001b] are used to calculate the chemical loss of CO in the forward model.

[8] Spatial and temporal patterns of emissions are prescribed in the forward model, representing direct emissions of CO and approximating the atmospheric chemical production of CO from short-lived natural and anthropogenic nonmethane hydrocarbons (NMHC). Emissions of CO from fuel-use and tropical biomass-burning are based on the EDGAR/GEIA inventory [*Olivier et al.*, 1996]. In specifying the biomass-burning source, the magnitude of emissions from agricultural waste burning is set at 25% [*Andreae*, 1991] of the EDGAR/GEIA inventory value to correct for the mistaken assumption made in the inventory that all agricultural residues are burnt. CO emissions from forest fires in the high northern latitudes and from biomass-burning in Australia, which are not included in the EDGAR/GEIA inventory, are specified based on burnt area statistics for these regions reported elsewhere [*Cooke and Wilson*, 1996]. The seasonality of tropical biomass-burning emissions is prescribed based on a published analysis of the geographical variation in fire season [*Galanter et al.*, 2000], while seasonality of emissions from forest fires in the high northern latitudes is based on compiled fire climatology statistics for Canada [*Harrington*, 1982].

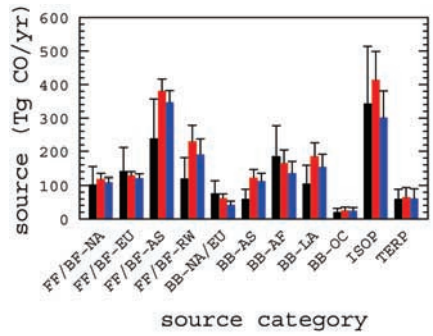

Figure 1. A priori and a posteriori estimates of CO sources for various source categories. A priori estimates are shown as black bars, and a posteriori estimates are shown as red (for the standard OH scenario) and blue (for the reduced OH scenario) bars. Error bars represent 1-sigma uncertainty. The a priori yield of CO from CH_4 oxidation is assumed to be 0.85 ± 0.05 mole of CO per mole of CH_4 oxidized. The calculated a posteriori yields are 1.0 ± 0.04 and 0.93 ± 0.04 mole CO per mole CH_4 oxidized for the standard and reduced OH scenarios, respectively. The global magnitudes of the a priori CO source from CH_4 oxidation are 808 and 647 Tg CO yr^{-1} for the standard and reduced OH scenarios, respectively. The corresponding a posteriori source magnitudes are 949 and 709 Tg CO yr^{-1}.

[9] Chemical production of CO from short-lived NMHC is included in the model as equivalent emissions of CO from the appropriate source category, based on anthropogenic [*Olivier et al.*, 1996] and natural NMHC emission inventories [*Guenther et al.*, 1995] and values of CO chemical yields from the oxidation of these compounds [*Altshuler*, 1991; *Hatakeyama et al.*, 1991; *Miyoshi et al.*, 1994]. CO chemical production from CH_4 oxidation is calculated in the model using the prescribed OH fields and prescribed CH_4 fields (90S-30S: 1672 ppbv; 30S-EQ: 1681 ppbv; EQ-30N: 1737 ppbv; 30N-90N: 1794 ppbv).

3. Results

[10] Figure 1 shows the a priori (i.e., bottom-up) and a posteriori (i.e., top-down) estimates of CO source strengths and uncertainties for each of the source categories considered. The top-down and bottom-up estimates differ by 110–140 Tg CO yr^{-1} for the FF/BF-AS and FF/BF-RW source categories, and by 60–80 Tg CO yr^{-1} for the BB-AS, BB-LA, and ISOP source categories. The mean a posteriori estimate of the CO yield from CH_4 oxidation (METH source category) is unity. It is worth noting here that the a priori FF/BF source estimates shown in Figure 1 are derived from the EDGAR/GEIA inventories that are representative of the early 1990s, while the a posteriori estimates are derived using atmospheric measurements for 1994. The extent to which growth in fossil-fuel and biofuel use

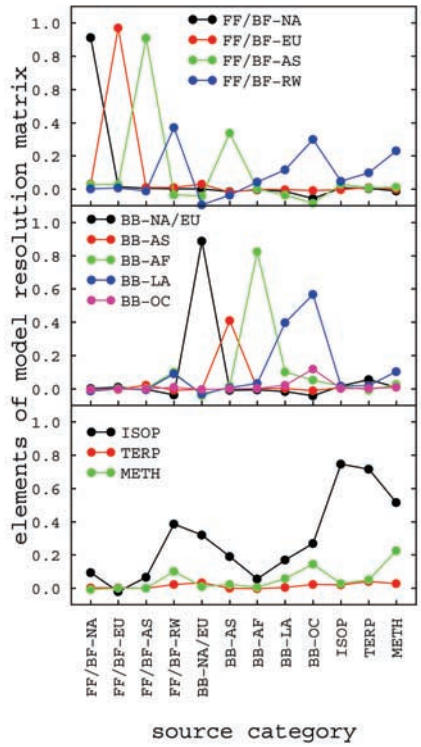

Figure 2. Elements of the data resolution matrix **A**. In each panel, filled circles represent individual elements of **A**. Different colors are used to distinguish elements of different rows of **A** with the corresponding columns indicated on the x-axis. Lines connecting the points are drawn for clarity and have no physical significance.

between 1990 and 1994 accounts for the differences shown in Figure 1 is examined later in the text.

[11] Characterizing the sensitivity of the a posteriori source estimates to the unknown true magnitudes of the individual sources is an important component of inverse analysis. This is accomplished by considering the model resolution matrix **A** = **GK** (analogous to the averaging kernel matrix in remote sounding applications), element A_{ij} of which provides information on the sensitivity of the estimated magnitude of source category 'i' to the unknown true magnitude of source category 'j' [*Rodgers*, 2000]. In the ideal case, **A** would be an identity matrix. Figure 2 shows the calculated elements of **A**, with individual lines corresponding to the individual rows of **A**. It is apparent from Figure 2 that the FF/BF-NA and FF/BF-EU source categories are well constrained by the measurements. The same is true for the FF/BF-AS source category, with the caveat that the measurements do not uniquely differentiate between this category and the BB-AS category. As a result, the calculated a posteriori uncertainty for the FF/BF-AS source category (±36 Tg CO yr^{-1}) is larger than the uncertainties for the FF/BF-NA and FF/BF-EU categories (±12–15 Tg CO yr^{-1}). Figure 2 also shows that the other source categories for which relatively large differences are seen between the a priori and a posteriori source estimates (FF/BF-RW, BB-AS, BB-LA, ISOP, and METH) are not uniquely constrained by the measurements. We also find that the collocation of the FF and BF CO sources in Asia does not permit us to differentiate between these sources.

[12] The improvement in model performance when a posteriori sources are used is evident in Figure 3, which shows comparisons between observed and modeled monthly-mean CO for selected sites. Two additional aspects of this figure are noteworthy. First, even at sites downwind of Asia (SCSN15, MID, KUM), sources other than the FF/BF-AS source are important, leading to a disproportionately small (but nevertheless significant) impact of the large change in this source category. Second, the model significantly underestimates CO mixing ratios in the remote Pacific in winter and spring even with the higher a posteriori source estimates, indicating that important inconsistencies remain in our understanding of the factors that shape the tropospheric CO distribution in this region.

[13] The prescribed OH concentration fields can be scaled downward by 10–20% and remain consistent with the estimated lifetime of methylchloroform against the tropospheric OH sink [*Spivakovsky et al.*, 2000; *Bey et al.*, 2001b]. To test the effect of a change of this magnitude, a forward model simulation was performed with OH concentrations uniformly reduced by 20% and the results from this simulation were used in the inversion analysis. The computed source estimates for this scenario are also shown in Figure 1. It is evident that the a posteriori estimate for the FF/BF-AS category changes only modestly in response to the change in the prescribed OH fields.

[14] On a global basis, the a priori source estimates (including the source from CH_4 oxidation) total 2261 and

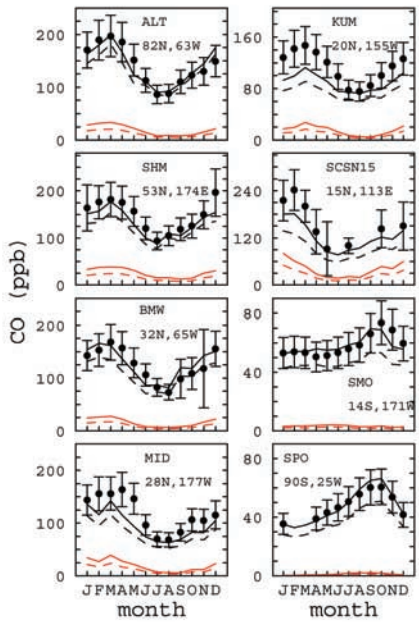

Figure 3. Comparisons of observed (black circles) and modeled monthly-mean CO concentrations using a priori (dashed lines) and a posteriori (solid lines) source estimates at selected sites. Contributions from the FF/BF-AS category (red lines) to total modeled CO (black lines) are shown. Error bars represent 1-sigma uncertainty. Site codes in each panel correspond those listed in *Novelli et al.* [1998]. The latitude-longitude location of the site is also identified.

2100 Tg CO yr^{-1} for the standard and reduced OH scenarios, respectively. The corresponding global burdens with the a priori sources are 320 and 368 Tg CO, respectively. The global a posteriori source estimates total 2846 and 2306 Tg CO yr^{-1} for the standard and reduced OH scenarios, respectively. The corresponding global burdens with the a posteriori sources are 397 and 399 Tg CO, respectively. On an annual and global basis, the total CO source is balanced by the OH oxidation sink. The global- and annual-average CO lifetimes are 1.7 and 2.1 months for the standard and reduced OH scenarios respectfully.

4. Discussion and Conclusions

[15] Our best estimate of the CO source associated with the FF/BF-AS category is 350–380 Tg yr^{-1} (with a 1-sigma uncertainty of ±35 Tg yr^{-1}) out of a global source of 780–860 Tg yr^{-1} from fossil-fuel and biofuel combustion. There is thus a discrepancy of 110-140 Tg yr^{-1} between top-down and bottom-up estimates of the CO source associated with fuel-use in Asia. It is worth noting that the a priori estimate of the total direct emissions of CO from fossil-fuel and biofuel combustion in Asia used here is similar to an independent bottom-up source estimate for Asia [*Streets and Waldhoff*, 1999], despite differences in the breakdown within individual sectors in the source category. Emissions of CO from fuel-use in China, a country which accounts for a significant fraction of total Asian emissions [*Streets and Waldhoff*, 1999] and where there has been a rapid growth in the industrial and transportation sectors [*Streets and Waldhoff*, 2000], are estimated to have increased by only 16 Tg yr^{-1} between 1990 and 1995 due to almost no change in the relatively large biofuel combustion source [*Streets and Waldhoff*, 2000]. Thus it is also unlikely that a significant portion of the discrepancy between the top-down and bottom-up estimates in Asia can be explained by growth in Asian CO emissions from 1990 (the reference year for the bottom-up estimate) to 1994 (the reference year for the top-down estimate). Our results are also consistent with the modeling study of *Bergamaschi et al.* [2000a] that suggested that the global CO source from fuel-use is higher than present inventory estimates, assuming similar distribution of natural sources to that considered here.

[16] The discrepancy between the top-down and bottom-up source estimates for the FF/BF-AS category points to an important gap in our understanding of the global atmospheric CO budget. Our analysis implies that the quantity of fuel consumed in Asia and/or the associated CO emission factors are systematically underestimated in current inventories. To the extent that fuel use in Asia is underestimated in current inventories, our study has broader implications for global atmospheric chemical budgets since anthropogenic CO emissions are often closely coupled to emissions of other radiatively and chemically important trace gases and aerosols. In addition to the global budget perspective, there is a policy-relevant need for resolving regional emission budgets of CO as an important first step towards characterizing the potentially significant impact of individual source regions on air quality in downwind regions. There is thus a need for fully reconciling the differences between the top-down and bottom-up estimates of CO emissions from fuel combustion in Asia, developing robust estimates of CO emissions from other source categories, and resolving remaining inconsistencies between source estimates and measured atmospheric concentrations of CO.

[17] **Acknowledgments.** This work was supported by the NASA ACMAP and EOS/IDS programs. The CO measurements were made with support from the NOAA Climate and Global Change Program – Radiatively Important Trace Species. Computer resources were provided by the North Carolina Supercomputing Center. Constructive comments on the original manuscript from two anonymous referees are acknowledged.

References

Altshuler, A. P., The production of carbon monoxide by the homogeneous NO_x-induced photooxidation of volatile organic compounds in the troposphere, *J. Atmos. Chem.*, *13*, 155–182, 1991.

Andreae, M. O., Biomass burning: Its history, use, and distribution and its impact on environmental quality and global climate, in *Global Biomass Burning: Atmospheric, Climatic, and Biospheric Implications*, edited by J. S. Levine, pp. 3–21, The MIT Press, Cambridge, Massachusetts, 1991.

Bergamaschi, P., et al., Inverse modeling of the global CO cycle 1. Inversion of CO mixing ratios, *J. Geophys. Res.*, *105*, 1909–1927, 2000a.

Bey, I., et al., Global modeling of tropospheric chemistry with assimilated meteorology: Model description and evaluation, *J. Geophys. Res.*, *106*, 23,073–23,095, 2001b.

Cooke, W. F., and J. J. N. Wilson, A global black carbon aerosol model, *J. Geophys. Res.*, *101*, 19,395–19,409, 1996.

Galanter, M., et al., Impacts of biomass burning on tropospheric CO, NO_x, and O_3, *J. Geophys. Res.*, *105*, 6633–6653, 2000.

Granier, C., et al., A three-dimensional study of the global CO budget, *Chemosphere: Global. Change Sci.*, *1*, 255–261, 1999.

Guenther, A., et al., A global model of natural volatile organic compound emissions, *J. Geophys. Res.*, *100*, 8873–8892, 1995.

Harrington, J. B., *A statistical study of area burned by wildfire in Canada 1953–1980*, Report F046-11/16-1982E, Canadian Forestry Service, Environment Canada, Ontario, 1982.

Hatakeyama, S., et al., Reactions of OH with a-pinene and b-pinene in air: Estimate of global CO production from the atmospheric oxidation of terpenes, *J. Geophys. Res.*, *96*, 947–958, 1991.

Holloway, T., H. Levy II, and P. Kasibhatla, Global distribution of carbon monoxide, *J. Geophys. Res.*, *105*, 12,123–12,147, 2000.

Kanakidou, M., and P. J. Crutzen, The photochemical source of carbon monoxide: Importance, uncertainties and feedbacks, *Chemosphere: Global. Change Sci.*, *1*, 91–109, 1999.

Logan, J. A., M. J. Prather, S. C. Wofsy, and M. B. McElroy, Tropospheric chemistry: A global perspective, *J. Geophys. Res.*, *86*, 7210–7254, 1981.

Miyoshi, A., S. Hatakeyama, and N. Washida, OH-radical initiated photooxidation of isoprene: An estimate of global CO production, *J. Geophys. Res.*, *99*, 18,779–18,787, 1994.

Novelli, P. C., K. A. Masarie, and P. M. Lang, Distributions and recent changes in carbon monoxide in the lower troposphere, *J. Geophys. Res.*, *103*, 19,015–19,033, 1998.

Olivier, J. G. J., et al., *Description of EDGAR Version 2.0: A set of global emission inventories of greenhouse gases and ozone-depleting substances for all anthropogenic and most natural sources on a per country basis and on 1° x 1° grid*, Report 771060002, National Institute of Public Health and the Environment (RIVM), The Netherlands, 1996.

Rodgers, C. D., *Inverse Methods for Atmospheric Sounding: Theory and Practice*, World Scientific Publishing Co. Pte. Ltd., Singapore, 2000.

Spivakovsky, C. M., et al., Three-dimensional climatological distribution of tropospheric OH: Update and evaluation, *J. Geophys. Res.*, *105*, 8931–8980, 2000.

Streets, D. G., and S. T. Waldhoff, Greenhouse-gas emissions from biofuel combustion in Asia, *Energy*, *24*, 841–855, 1999.

Streets, D. G., and S. T. Waldhoff, Present and future emissions of air pollutants in China: SO_2, NO_x, and CO, *Atmos. Environ.*, *34*, 363–374, 2000.

P. Kasibhatla and A. Arellano, Nicholas School of the Environment and Earth Sciences, Duke University, Durham, NC 27708, USA. (psk9@duke.edu; afa3@duke.edu)

J. A. Logan and P. I. Palmer, Division of Engineering and Applied Sciences, Harvard University, Cambridge, MA 02138, USA. (jal@io.harvard.edu; pip@io.harvard.edu)

P. Novelli, Climate Monitoring and Diagnostics Laboratory, NOAA, Boulder, CO 80305, USA. (pnovelli@cmdl.noaa.gov)